

*Med Chem.* Author manuscript; available in PMC 2013 January 26.

Published in final edited form as:

J Med Chem. 2012 January 26; 55(2): 735–742. doi:10.1021/jm201238p.

# Discovery and Synthesis of Namalide Reveals a New Anabaenopeptin Scaffold and Peptidase Inhibitor

Pradeep Cheruku<sup>†</sup>, Alberto Plaza<sup>†</sup>, Gianluigi Lauro<sup>‡</sup>, Jessica Keffer<sup>†</sup>, John R. Lloyd<sup>†</sup>, Giuseppe Bifulco<sup>\*,‡</sup>, and Carole A. Bewley<sup>\*,†</sup>

<sup>†</sup>Laboratory of Bioorganic Chemistry, National Institute of Diabetes and Digestive and Kidney Diseases, National Institutes of Health, Bethesda, Maryland 20892

<sup>‡</sup>Dipartimento di Scienze Farmaceutiche e Biomediche, University of Salerno, Via Ponte Don Melillo, 84084 Fisciano, Salerno, Italy

#### **Abstract**

The discovery, structure elucidation and solid phase synthesis of namalide, a marine natural product, are described. Namalide is a cyclic tetrapeptide; its macrocycle is formed by only three amino acids, with an exocyclic ureido phenylalanine moiety at its C-terminus. The absolute configuration of namalide was established and analogs generated through Fmoc-based solid phase peptide synthesis. We found that only natural namalide and not its analogs containing L-Lys or L-allo-Ile inhibited carboxypeptidase A at submicromolar concentrations. In parallel, an Inverse Virtual Screening approach aimed at identifying protein targets of namalide selected carboxypeptidase A as the third highest scoring hit. Namalide represents a new anabaenopeptin-type scaffold, and its protease inhibitory activity demonstrates that the 13-membered macrolactam can exhibit similar activity as the more common hexapeptides.

#### Introduction

The diversity of natural products coming from marine invertebrates and possessing interesting biological activities has been well documented, yet discovery of new compounds and their associated modes of action continues apace. To mention only a few examples, marine natural products that can inhibit biological targets linked to cancer, and bacterial cell division have been reported. Here we describe the identification and Fmoc-based solid phase synthesis of a new ureido-containing cyclic peptide, namalide (1), a potent inhibitor of carboxypeptidase A (CPA). Namalide was isolated from the same collection of the marine sponge *Siliquariaspongia mirabilis* that provided the anti-HIV lipopeptides mirabamides A–D, the antitumor polyketide mirabalin, and the known antifungals aurantosides A–B. Namalide represents a new anabaenapeptintype scaffold possessing a 13-membered macrolactam core. Inverse virtual screening and molecular docking of this novel scaffold are consistent with observed protease inhibition and selectivity.

<sup>\*</sup>To whom correspondence should be addressed: bifulco@unisa.it, caroleb@mail.nih.gov..

#### Results

### Isolation and Structure Elucidation of Namalide (1)

Previously we reported the discovery of three separate classes of natural products coming from the aqueous extract of a single collection of the marine sponge S. mirabilis. 8-10 Mirabamides, mirabalin and aurantosides were isolated from the *n*-BuOH fraction of the aqueous extract after fractionation on a Sephadex LH-20 column eluting with MeOH followed by HPLC purification. During these studies, we detected a separate group of Sephadex fractions containing what appeared to be a novel compound on the basis of its molecular weight (ESI-MS). In addition, these fractions showed strong inhibition of the enzyme CPA. Active fractions were combined and purified by C12 RP-HPLC to give just 0.4 mg of the active compound (~90% pure), a new natural product named namalide (1, Figure 1). Shown by HR-ESI-MS, compound 1 had a molecular formula of C<sub>31</sub>H<sub>41</sub>N<sub>5</sub>O<sub>6</sub> (m/  $z 602.2955 \text{ [M+Na]}^+$ , calcd for C<sub>31</sub>H N<sub>5</sub>NaO<sub>6</sub>, 602.2955) requiring 14 of unsaturation. A <sup>1</sup>H-<sup>13</sup>C HSQC spectrum (CD<sub>3</sub>OD) showed correlations for four methine signals resonating between  $\delta_H$  3.95–4.57 and  $\delta_C$  55.9–61.3, suggesting that  $\boldsymbol{1}$  was a peptide containing four α-amino acids. 2D NMR data including HSQC, HMBC, HOHAHA, and DQF-COSY spectra revealed the presence of isoleucine, lysine, and two phenylalanine residues (Table 1). A pair of HMBC correlations from H-2<sub>Phe2</sub> ( $\delta_H$  4.42) and H-2<sub>Lvs</sub> ( $\delta_H$ 4.00) to an unassigned carbon at  $\delta_C$  159.4 suggested the presence of a ureido group that must join Phe2 to Lys, and account for the remaining CO group indicated by the molecular formula.

Additional long-range H–C correlations from the  $\epsilon$ -methylene protons of lysine ( $\delta_H$  3.63, 2.86,  $\delta_C$  38.2) to the carbonyl at  $\delta_C$  172.9 (C-1<sub>Phe1</sub>), and from the  $\alpha$ -proton of Phe1 ( $\delta_H$  4.57) to the carbonyl resonance at  $\delta_C$  173.7 (C-1<sub>Ile</sub>) completed the linear sequence of **1**. Although the molecular formula requires **1** to be a cyclic peptide, long-range correlations that would connect the amino group of Ile to the carboxy group of either Lys or Phe2 were not observed in CD<sub>3</sub>OD or DMSO- $d_6$  spectra. Residue connectivity could be established, however, from a ROESY spectrum of **1** in DMSO- $d_6$  (Table S1, Supporting Information). In particular a strong correlation between the amide proton at  $\delta_H$  7.17 (NH<sub>Ile</sub>) and the  $\alpha$ -proton of Lys at  $\delta_H$  3.78 (H-2<sub>Lys</sub>) indicated that **1** comprised a three-residue macrocycle *N*-linked to an exocyclic Phe residue via a ureido bridge. Thus namalide bears similarities to the anabaenapeptin family of peptides, but is unprecedented in its tripeptide macrocycle.

Independent evidence for the presence and placement of the ureido-Phe moiety was provided by ESIMS<sup>n</sup> experiments. Fragmentation of the major ion peak at m/z 602 [M+Na]<sup>+</sup> displayed ion fragments at m/z 437 [M+Na-Phe]<sup>+</sup> and m/z 409 [M+Na-Phe-CO]<sup>+</sup> corresponding to loss of Phe and Phe-CO, respectively. Further MS<sup>4</sup> fragmentation of the daughter ion at m/z 409 yielded a minor ion fragment at m/z 262 [M+Na-Phe-CO-Phe]<sup>+</sup>. These fragmentation patterns were consistent with our NMR results.

The absolute configurations of the alpha carbons for both Phe residues and Ile were readily established as L from LC-MS analyses of the L- and D- FDLA (1-fluoro-2,4-dinitrophenyl-5-L/D-leucinamide) derivatives of an acid hydrolysate of 1, in conjunction with comparison of retention times with authentic standards. However, due to our limited material or the limitations of the method, this analysis did not allow us to confidently assign the configuration of the Lys residue and C-3 of Ile. Worth noting, although all anabaenapeptin-type compounds derived from cyanobacteria contain D-Lys exclusively, 12,13 peptides reported to contain L-Lys rather than D have been isolated from marine sponges. 14–17 To address these unknowns and provide additional compound for biological screening, we developed a synthetic route to provide namalide and its stereoisomers.

#### Solid-Phase Synthesis of Namalide and Analogs

When designing the synthesis, we sought to develop a route that would be amenable to standard Fmoc-based SPPS conditions, including on-resin construction of the urea moiety.  $^{18}$  To allow coupling to the free amine of the growing peptide chain, the exocyclic C-terminal residue must be coupled to the resin through its free carboxylic acid. A retrosynthetic analysis of 1 suggested macrolactamization should occur between the amino group of Ile and the carboxy group of Lys (Scheme 1) with chain elongation occurring through the side chain  $\epsilon$  amino group of Lys.

The synthesis began with preparation of the reactive 4-nitrophenylcarbamate derivative of lysine (2) by treatment of *N*ε-Fmoc-protected Lys with allyl bromide followed by 4-nitrophenylchloroformate to give the carbamate in good yield (Supporting Information), an approach used in the synthesis of the cyanobacterial metabolite oscillamide Y. <sup>18</sup> Following deprotection of Fmoc-<sub>L</sub>-Phe-Wang resin, the free amine was treated with 2 in the presence of Hunig's base to construct the urea moiety. Standard Fmoc-based SPPS using O-benzotriazole-N,N,N',N'-tetramethyl-uronium-hexafluoro-phosphate (HBTU) and hydroxybenzotriazole (HOBt) as coupling reagents furnished the protected linear peptide on resin (Scheme 2). Palladium (0) mediated removal of the allyl group followed by Fmoc deprotection with 20% piperidine gave the unprotected linear precursor for on-resin cyclization.

Macrolactamization was first carried out using benzotriazol-1-yl-oxytripyrrolidinophosphonium hexafluorophosphate (PyBOP) and HOBt. <sup>19</sup> Product formation at 20 min and 1, 2, 3, 6 and 18 h time points was monitored by LC-MS analysis of the cleavage products of 5 mg resin aliquots. We found that conversion of the linear precursor to the natural product occurred in highest yield after 3 h. Longer reaction times using PyBOP/HOBt gave rise to other unidentified products having incorrect masses. Surprisingly LC-MS analysis of the cleavage mixtures showed that formation of a product with m/z 1158, twice that of 1, was formed in an approximate 1:1 ratio relative to the desired product during the course of the cyclization. Proton NMR of the product showed a single set of peaks that would account for half the detected mass, thereby indicating the product 3 to be a symmetrical namalide dimer. Thus inter strand coupling must occur during the on-resin cyclization to lead to formation of 3.

Macrocyclization in the presence of other coupling reagents including bromo-trispyrrolidino phosphoniumhexafluorophosphate (PyBrOP)/HOBt, diisopropylcarbodiimide (DIC)/HOBt, HBTU/HOBt, and HATU/HOBt was also tested. In the presence of the stronger activator PyBrOP/HOBt, the dimeric product was formed to the exclusion of the monomeric one. For the remaining three coupling reagents cyclization occurred more slowly than with PyBOP/HOBt, and no improvement in the monomer:dimer ratio was observed. Subsequent cleavage of the cyclic peptide from the solid support using TFA:H<sub>2</sub>O (9:1) followed by reverse phase HPLC purification of the crude peptide afforded 4.6 mg of 1 in an overall yield of 8% on a scale of 0.1 mmol.

To establish configurations at C-3 of Ile and C-2 of Lys, two additional namalide analogs containing L-Ile/L-Lys and L-allo-Ile/D-Lys (**4**, **5**, Figure 2) were synthesized using the same SPPS strategy with appropriate amino acid precursors. Comparisons of the NMR spectra and RP-HPLC retention times of the three synthetic peptides **1**, **4** and **5** with that of the natural product showed that the isomer containing D-Lys and L-Ile corresponded to the natural material.

#### **Bioactivity of Namalide and Analogs**

Members of the anabaenopeptin<sup>20</sup> family of cyclic peptides are known to inhibit carboxypeptidases and other proteases.<sup>21–24</sup> Although a high-resolution structure of an anabaenopeptin-type peptide in complex with any carboxypeptidase has not been determined, selectivity profiles of natural products and synthetic analogs provide good evidence that the C-terminal ureido amino acid confers specificity toward different proteases.<sup>24,25</sup> Peptides 1, 3, and 4–7 (Figure 2) were evaluated as inhibitors of bovine pancreas CPA using *N*-(4-methoxyphenylazoformyl)phenylalanine as a colorimetric substrate in a 96 well plate format. The results are summarized in Table 2.

The synthetic version of natural namalide (1) containing  $_{\rm D}$ -Lys and  $_{\rm L}$ -Ile was the most potent inhibitor of CPA with an IC $_{50}$  value of 250±30 nM. Peptide 4, the corresponding  $_{\rm L}$ -Lys analog was inactive at concentrations as high as 30  $\mu$ M, and analog 5 bearing  $_{\rm L}$ -allo-Ile/ $_{\rm D}$ -Lys appeared to be inactive, although its insolubility yielded poor assay results. The linear version of namalide, 6, showed an 18-fold reduction in activity relative to 1 with an IC $_{50}$  value of 4.5  $\mu$ M. In contrast cyclic tripeptide 7, which lacks the C-terminal exocyclic ureido Phe, and the namalide dimer 3 were inactive. For comparison, compounds 1, 4, 6 and 7 were tested against carboxypeptidase U (CPU), also known as activated thrombin-activable fibrinolysis inhibitor (TAFIa), an enzyme known to recognize C-terminal basic amino acids in its S1 pocket; <sup>25</sup> and  $\alpha$ -chymotrypsin, a serine protease that recognizes aliphatic and aromatic amino acids. <sup>26</sup> None of these peptides inhibited either enzyme at concentrations as high as 60  $\mu$ g/mL. Together these results demonstrate the importance of the lysine configuration for CPA inhibition in this new tricyclic peptide scaffold. The lack of inhibitory activity of the des-ureido-Phe analog 7 further suggests that namalides may inhibit through a similar mode of binding as the larger anabaenapeptin-type compounds.

#### Inverse Virtual Screening and Molecular Docking of Namalide

Because namalide represents a new natural product scaffold, we were interested in applying our recently described Inverse Virtual Screening in silico approach<sup>27</sup> using Autodock Vina software<sup>28</sup> to assist in identifying other possible new targets of namalide. In this method, a database of known protein structures is searched to identify complementary ligand binding partners on the basis of calculated binding energies relative to those for a set of known ligands.<sup>27</sup> For docking calculations, a three-dimensional model of namalide was prepared by performing combined Monte Carlo conformational searches and molecular dynamics simulations, followed by energy and geometry minimization of the obtained structure. The minimized model was used against a panel of 159 receptors involved in cancer processes and whose coordinates were extracted from the Protein Data Bank (Tables S3 and S4, Supporting Information). For normalization of the results a pre-built matrix containing the affinity values of a library of 22 natural compounds (used as 'blanks') with structural and molecular weight properties similar to those of 1 was employed (Table S3, Supporting Information). In particular we calculated an average value of binding energy for each target receptor on all of the compounds in the matrix and then normalized the affinity values of 1 using the equation:

$$V=V_o/V_R$$
 [1]

where V is the normalized value of binding energy,  $V_0$  is the value of binding energy before the normalization and  $V_R$  is the average value of binding energy for each targets.

We were gratified to find that of the 159 proteins screened, CPA was identified as the third best hit on the basis of normalized binding energy (Table S5, Supporting Information).<sup>29</sup> As

shown in Figure 3, molecular docking of **1** to CPA using Autodock 4.2<sup>30</sup> places the C-terminal carboxylate in close proximity to the Zn<sup>2+</sup> atom, and within hydrogen bonding distance with the guanidine groups of Arg 127 and Arg 145, key residues in the active site and specificity pocket of CPA,<sup>26,31</sup> as well as the side chain of Asn 144. Additional interactions are seen between the amide of Ile and the hydroxyl of Tyr 248. Similarly the ureido group is involved in electrostatic interactions with Arg 127 and Tyr 248. Despite its reduced size relative to the pentapeptide core of anabaenapeptins, both electrostatic and aliphatic interactions are observed between CPA and residues in the cyclic portion of **1** in the docked model. In particular, the side chain of p-Lys is positioned close to Phe 279, and the amide of Ile is hydrogen bonded to the OH of Tyr 248. Consistent with other models and the biological activity, the C-terminal Phe is directed toward the hydrophobic specificity pocket formed in part by Ile247, Tyr 248 and Ala 250.

To investigate the specificity of namalide for CPA, we performed molecular docking of **4**, the L-Lys-containing analog, to CPA; and of **1** to CPU using the same protocol as above. In the lowest energy model of **4** bound to CPA, interactions between the exocyclic Phe and its carboxylate group with CPA are preserved. However, the inverted configuration of Lys results in a flipping of the ring which moves the ureido group further from the Zn<sup>2+</sup> atom and reduced interactions between the ring amino acids and CPA (*cf.* Supporting Information, Figures S1 and S2). Docking of **1** to CPU failed to give any reasonable models with **1** bound to or near the active site (*cf.* Supporting Information, Figure S3). Both CPU and carboxypeptidase B are exopeptidases that preferentially cleave basic C-terminal residues, recognizing Arg and Lys as opposed to the aromatic residues preferred by CPA. The lack of inhibitory activity toward CPU lends further support that this scaffold binds peptidases in a similar fashion to the larger anabaenapeptins. <sup>12,22</sup>

In summary, we have discovered a new mini-anabaenopeptin scaffold from a marine sponge. Structure elucidation and synthesis of the natural product establish the absolute configuration of all amino acids as L, with the exception of D-Lys. In contrast to other anabaenopeptins, the macrocycle comprises just three rather than the typical five amino acids, leading to a 13-membered macrolactam ring versus the usual 19-membered one. The presence of this strained ring likely accounts for the side product of a namalide dimer formed during the on-resin cyclization employed in the synthesis of 1. In keeping with specificity patterns described for a few peptides of this class, the carboxypeptidase inhibitory activity depends on the presence of D-Lys, and the exocyclic amino acid appears to dictate specificity. Because namalide inhibits CPA with potencies comparable to the more common hexapeptides, it will be interesting to evaluate other designed namalide analogs against CPA and related hydrolases.

# **Experimental Section**

#### **Sponge Material**

The sponge was collected from open reef off Nama Island, southeast of Chuuk lagoon, in the Federated States of Micronesia, at a depth of 50 m, on 25 August 1994. The sponge was identified previously<sup>8</sup> to be most closely comparable to *Siliquariaspongia mirabilis* (de Laubenfels, 1954) (Lithistid Demospongiae: Family Theonellidae), but lacks the characteristic non-articulated tetracladine desmas that characterize the genus. A voucher specimen has been deposited at the Natural History Museum, London, United Kingdom (BMNH 2007.7.9.1). Samples were frozen immediately after collection, and shipped on dry ice to Frederick, MD, where they were freeze-dried and extracted with H<sub>2</sub>O (OCDN 2547).

#### **Experimental Details for Extraction and Isolation**

A 6 g portion of the extract was partitioned with  $n\text{-BuOH-H}_2O$  (1:1) to afford a dried n-BuOH extract (0.7 g) that was fractionated on a Sephadex LH-20 column (50 × 2.5 cm) using MeOH as mobile phase. Fractions containing peptides were combined and the solvent removed in vacuo to give 16 mg of a pale orange film containing the peptide and the known compounds aurantosides,  $^{10}$  orange colored polyenes. Purification by reverse-phase HPLC (Jupiter Proteo C12,  $250 \times 10$  mm, 90 Å,  $4\mu$  particle size, diode array detection at 220 and 280 nm) eluting with a linear gradient of 50-80% MeOH in 0.05% TFA in 50 min yielded compound 1 (0.4 mg,  $t_R=14.8$  min). Trace amounts of aurantosides remained in this final fraction where further separation was limited due to limited quantities of material.

#### **Experimental Details for Solid Phase Peptide Synthesis**

Solid-phase peptide synthesis was carried out manually on 0.1 mmol scale for 1; 0.05 mmol scale for 4, 5 and 7; and 0.25 mmol scale for 6, in solid phase peptide synthesis vessels with fritted glass supports under N<sub>2</sub> (1 atm) using the following conditions: resins (100–200 mesh, 0.61 meq, 0.16 g, 0.1 mmol) were immersed in CH<sub>2</sub>Cl<sub>2</sub> (10 mL) and agitated for 2 h to allow for swelling, drained and washed with DMF (2 × 5 mL). Fmoc protecting groups were removed by treating the resin with a solution of 20% piperidine/DMF (5 mL) for 30 min, followed by washing with DMF (5  $\times$  5 mL), CH<sub>2</sub>Cl<sub>2</sub> (5  $\times$  5 mL) and DMF (5  $\times$  5 mL). For coupling reactions, an appropriate Fmoc-protected amino acid (4 equiv) was preactivated in the presence of HBTU (3 equiv) and DIPEA (8 equiv) in 10 mL DMF for 10 min, and the resulting solution added to the resin and agitated under N<sub>2</sub> for 2 h followed by washing with DMF (5  $\times$  5 mL), CH<sub>2</sub>Cl<sub>2</sub> (5  $\times$  5 mL) and DMF (5  $\times$  5 mL). For ureidocontaining peptides, the resin was suspended in 5 mL DMF, and a solution of 4nitrophenyloxycarbonyl-D-Lys(Fmoc)-OH allyl ester (2, Supporting Information) (173 mg, 0.32 mmol, 3eq) in DMF (5 mL) and DIPEA (0.11 mL, 0.6 mmol, 6eq) was added to the resin slurry, followed by shaking for 1.5 h. The resin was then washed with DMF ( $5 \times 5$ mL),  $CH_2Cl_2$  (5 × 5 mL) and DMF (5 × 5 mL). Following each coupling reaction, an ~5 mg aliquot of resin was cleaved and analyzed by LC-MS to monitor extent of the reaction. Following each coupling step, resin was treated with a solution of 20% Ac<sub>2</sub>O in DMF (10 mL) for 30 min and washed with DMF (5 × 5 mL) and CH<sub>2</sub>Cl<sub>2</sub> (5 × 5 mL). Cleavage From Resin: products were cleaved from the solid support by treatment with TFA:H<sub>2</sub>O (90:10, 10 mL) for 3 h. The resin was filtered and washed with TFA  $(2 \times 5 \text{ mL})$  and CH<sub>2</sub>Cl<sub>2</sub>  $(2 \times 5 \text{ mL})$ mL). The combined filtrate and washes were removed in vacuo to give the crude peptide, which was suspended in CH<sub>3</sub>CN/H<sub>2</sub>O (1:1) and lyophilized. Purification of the crude material was carried out by RP HPLC and the purity of compounds used in the biological assays was ≥95% as determined by RP-HPLC (Table S2 of the Supporting Information)

#### **Experimental Details for Other Synthetic Procedures**

Deprotection of Alloc Ester: after coupling of the final amino acid followed by capping, the resin was treated with a solution of tetrakis(triphenylphosphine) palladium (0) (116 mg, 0.1 mmol) and dimedone (140 mg, 1.0 mmol) in dry DMF o/n. The reaction vessel was protected from light during the course of deprotection, after which the resin was washed with CH<sub>2</sub>Cl<sub>2</sub> (5 × 5 mL), DMF (5 × 5 mL), 0.5% DIPEA + 0.5% diethyldithiocarbamic acid sodium salt in DMF (5 × 5 mL), DMF (5 × 5 mL), and CH<sub>2</sub>Cl<sub>2</sub> (5 × 5 mL). On-Resin Cyclization: a solution of PyBOP (280 mg, 0.6 mmol), HOBt (81 mg, 0.6 mmol) and DIPEA (0.1 mL, 0.6 mmol) in CH<sub>2</sub>Cl<sub>2</sub>/DMF (1:1, 10 mL) was added to the resin and the mixture shaken for 3 h. The resin was washed with CH<sub>2</sub>Cl<sub>2</sub> (5 × 5 mL), DMF (5 × 5 mL), and CH<sub>2</sub>Cl<sub>2</sub> (5 × 5 mL).

#### **Enzyme Assays**

Peptides were tested for inhibition of CPA and chymotrypsin using respective colorimetric substrates N-(4-methoxyphenylazoformyl)-Phe-OH $^{33}$  and N-benzoyl-L-tyrosine ethyl ester, all of which were purchased from Sigma. Assays were performed in 96-well plates (CPA) and 10 mm quartz cuvette (chymotrypsin) at 25 °C, in the presence of 1 U enzyme and 10  $\mu$ L inhibitor (typically 1 mM in DMSO) or solvent (DMSO) in a final volume of 200  $\mu$ L. Absorbance was measured after 5 min incubation at 350 nm for CPA and 256 nm for chymotrypsin. For CPA, inhibition curves were plotted and best fit to the equation %inhibition=100/(1+[inhibitor]/IC $_{50}$ ) using the program Kaleidagraph; no change in absorbance was observed for any of the peptides in the chymotrypsin assays. TAFIa/CPU enzyme assays were performed in a similar manner using the TAFIa kit from American Diagnostica according to the manufacturer's instructions.

**Synthetic Namalide (1)**—4.6 mg (yield = 8 %), colorless amorphous powder;  $[\alpha]_D^{24.5} = -41.8$  (c 0.03, DMSO/MeOH 1:3); IR (film)  $v_{max}$  3299, 2928, 2866, 1713, 1645, 1541, 1207, 1203, 1133, 698 cm<sup>-1</sup>; See Table S1 for NMR data; *HPLC analysis:* Jupiter 4 µm Proteo 90 Å LC Column  $100 \times 2$  mm, 220 nm (t = 0–5 min, 80% A, 20% B; t = 5–45 min, 20% A, 80% B, t = 46 min, 100% B. (A = water, 0.1% TFA, B = methanol). flow rate = 0.5 mL/min,  $t_R$ =36.28 min); HRMS (ESI): Calcd for  $C_{31}H_{42}N_5O_6$ : m/z,  $[M+H]^+$  580.3135. Found: 580.3139.

**Peptide 3 (dimeric 1)**—<sup>1</sup>H NMR (400 MHz, MeOD) δ 0.43 – 0.74 (m, 12H), 0.76 – 1.01 (m, 4H), 1.03 – 1.84 (m, 16H), 2.75 – 3.03 (m, 6H), 3.09 (m, 4H), 3.86 (brs, 2H), 3.97 (brs, 2H), 4.35 (brs, 2H), 4.49 (brs, 2H), 7.01 – 7.36 (m, 20H), 7.58 (brs, 2H), 7.89 (brs, 1H); *HPLC analysis:* Jupiter 4 μm Proteo 90 Å LC Column 100 × 2 mm, 220 nm (t = 0–5 min, 80% A, 20% B; t = 5–50 min, 10% A, 90% B, t = 51 min, 100% B. (A = water, 0.1% TFA, B = methanol). flow rate = 0.5 mL/min, t<sub>R</sub>=48.99 min); HRMS (ESI): Calcd for C<sub>31</sub>H<sub>42</sub>N<sub>5</sub>O<sub>6</sub>: m/z, [M + H]<sup>+</sup> 1159.6 Found: 1159.4.

**Peptide 4**—1.74 mg (yield = 6 %), colorless amorphous powder;  $[\alpha]_D^{26.5} = -23.0$  (c 0.1, DMSO/MeOH 1:1); IR (film)  $v_{max}$  3290, 2930, 2856, 1710, 1635, 1521, 1206, 1123, 695 cm<sup>-1</sup>; <sup>1</sup>H NMR (500 MHz, DMSO- $d_6$ ) δ 0.57 (d, J = 6.67 Hz, 3H), 0.72 (t, J = 7.26 Hz, 3H), 0.86 – 0.90 (m, 1H), 0.92 – 1.09 (m, 2H), 1.09 –1.20 (m, 1H), 1.20 –1.29 (m, 4H), 1.29 – 1.37 (m, 1H), 1.37 – 1.56 (m, 4H), 1.65 (brs, 1H), 2.70 – 2.87 (m, 2H), 2.94 – 3.12 (m, 2H), 3.91 (t, J = 9.32 Hz 1H), 4.01 – 4.08 (m, 1H), 4.31 (q, J = 7.45, 13.3 Hz 1H), 4.43 (q, J = 8.69, 15.96 Hz 1H), 6.22 (d, J = 8.10 Hz 1H), 6.44 (d, J = 8.19 Hz 1H), 7.14 – 7.23 (m, 6H), 7.23 – 7.32 (m, 4H), 7.46 (brs, 1H), 7.66 (d, J = 8.97 Hz 1H), 8.01 (d, J = 9.61 Hz 1H). HPLC analysis: Jupiter 4 μm Proteo 90 Å LC Column 100 × 2 mm, 220 nm (t = 0–5 min, 80% A, 20% B; t = 5–30 min, 20% A, 80% B, t = 35 min, 100% B. (A = water, 0.1% TFA, B = methanol). flow rate = 0.5 mL/min,  $t_R$ =35.89 min); HRMS (ESI): Calcd for  $C_{31}H_{42}N_5O_6$ : m/z,  $[M+H]^+$  580.3135. Found: 580.3145.

**Peptide 5**—2.6 mg (yield = 9 %), colorless amorphous powder;  $[a]_D^{26.7} = -51.6$  (c 0.06, DMSO/MeOH 1:1); IR (film)  $v_{max}$  3298, 2938, 2853, 1710, 1638, 1540, 1211, 1203, 1133, 698 cm<sup>-1</sup>; <sup>1</sup>H NMR (500 MHz, DMSO- $d_6$ ) δ 0.73 – 0.66 (m, 6H), 1.00 – 1.20 (m, 3H), 1.20 – 1.35 (m, 2H), 1.39 – 1.60 (m, 3H), 1.70 (brs, 1H), 2.68 – 2.85 (m, 2H), 2.91 (dd, J = 7.80, 13.3 Hz, 1H), 2.98 – 3.10 (m, 2H), 3.43 – 3.54 (m, 1H), 3.72 – 3.89 (m, 2H), 4.34 (dd, J = 7.83, 13.29 Hz, 1H), 4.40 (dd, J = 8.73, 15.3 Hz, 1H), 6.23 (d, J = 7.42 Hz 1H), 6.39 (d, J = 5.30 Hz, 1H), 7.05 – 7.08 (m, 1H), 7.08 – 7.37 (m, 10H), 7.45 (d, J = 7.80 Hz 1H), 7.56 (brs, 1H), 8.12 (d, J = 8.79 Hz, 1H). HPLC analysis: Jupiter 4 μm Proteo 90 Å LC Column 100 × 2 mm, 210 nm (t = 0–5 min, 80% A, 20% B; t = 5–45 min, 20% A, 80% B, t = 46 min,

100% B. (A = water, 0.1% TFA, B = methanol). flow rate = 0.5 mL/min,  $t_R$ =37.75 min); HRMS (ESI): Calcd for  $C_{31}H_{42}N_5O_6$ : m/z,  $[M + H]^+$  580.3135. Found: 580.3144.

**Peptide 6**—CLEAR amide resin (100–200 mesh, 0.49 meq, 0.2 g, 0.1 mmol) was immersed in CH<sub>2</sub>Cl<sub>2</sub> (10 mL) and agitated for 2 h. SPPS of **6** was carried out using the general protocol outlined above. The combined filtrate and washes were removed in vacuo to give the crude peptide, which was suspended in CH<sub>3</sub>CN/H<sub>2</sub>O (1:1) and lyophilized. Yield: 4.5 mg (30%), colorless amorphous powder;  $[\alpha]_D^{26.9} = +6$  (c 0.15 MeOH); IR (film) v<sub>max</sub> 3304, 2943, 2832, 2518, 1645, 1446, 1201, 1188 cm<sup>-1</sup>; <sup>1</sup>H NMR (500 MHz, DMSO- $d_6$ ) δ 0.71 (t, J = 6.40 Hz, 3H), 0.68 (d, J = 6.39 Hz, 3H), 0.93 – 1.14 (m, 2H), 1.14 –1.30 (m, 2H), 1.34 –1.60 (m, 4H), 1.63 – 1.78 (m, 4H), 2.23 –2.43 (m, 1H), 2.71 (t, J = 7.40 Hz, 2H), 2.81 – 2.93 (m, 2H), 3.02 – 3.10 (m, 2H), 4.03 (t, J = 6.91 Hz 1H), 4.16 (q, J = 6.73, 12.8 Hz, 1H), 4.32 –4.44 (m, 2H), 6.41 (d, J = 7.96 Hz, 1H), 6.52 (d, J = 6.76 Hz, 1H), 7.03 (d, J = 8.01 Hz, 1H), 7.19 – 7.30 (m, 6H), 7.12 – 7.19 (m, 4H), 7.57 (brs, 2H), 8.0 (t, J = 8.26 Hz, 2H). HPLC analysis: Jupiter 4 μm Proteo 90 Å LC Column 100 × 2 mm, 220 nm (t = 0–5 min, 80% A, 20% B; t = 5–45 min, 20% A, 80% B, t = 46 min, 100% B. (A = water, 0.1% TFA, B = methanol). flow rate = 0.5 mL/min, t<sub>R</sub>=32.13 min); HRMS (ESI): Calcd for C<sub>31</sub>H<sub>42</sub>N<sub>5</sub>O<sub>6</sub>: m/z, [M + H]<sup>+</sup> 597.3401 Found: 597.3412.

**Peptide 7**—Fmoc-Phe-Wang resin (100–200 mesh, 0.61 meg, 0.4 g, 0.25 mmol) was immersed in CH<sub>2</sub>Cl<sub>2</sub> (10 mL) and agitated for 2 h, and SPPS of the linear precursor carried out using the above protocol. The product was cleaved from the solid support by treatment with TFA: $H_2O$  (90:10, 15 mL) for 3 h. The resin was filtered and washed with TFA (2 × 5 mL) and CH<sub>2</sub>Cl<sub>2</sub> (2 × 5 mL). The combined filtrate and washes were removed in vacuo to give the linear peptide, which was suspended in CH<sub>3</sub>CN/H<sub>2</sub>O (1:1) and lyophilized. Cyclization: to a solution of linear peptide (20 mg, 0.15 mmol) in dry DMF (30 mL) was added PyBOP (140 mg, 0.3 mmol), HOBt (13 mg, 0.1 mmol) and DIPEA (0.1 mL, 0.6 mmol) in CH<sub>2</sub>Cl<sub>2</sub>/DMF (1:1, 10 mL) dropwise. The reaction mixture was allowed to stir for 4 h and the solvents were removed in vacuo. The crude Fmoc-protected cyclic peptide was purified by silica gel column chromatography followed by the removal of Fmoc in 20% piperidine/CH<sub>2</sub>Cl<sub>2</sub> (10 mL). Yield: 1.9 mg (10%), colorless amorphous powder;  $[\alpha]_D^{24.5}$  = -82 (c 0.05, DMSO/MeOH 1:1); IR (film)  $v_{max}$  3304, 2943, 2832, 2518, 1713, 1645, 1532, 1446, 1416, 1201, 1188 cm<sup>-1</sup>; <sup>1</sup>H NMR (500 MHz, DMSO- $d_6$ )  $\delta$  0.59 (d, J = 6.37 Hz, 3H), 0.79 (t, J = 7.26 Hz, 3H), 0.96 - 1.08 (m, 1H), 1.09 - 1.20 (m, 2H), 1.37 - 1.47 (m, 2H), 1.47-1.73 (m, 3H), 2.23-2.43 (m, 2H), 2.67-2.75 (m, 1H), 2.83 (dd, J=8.64 Hz 1H), 3.05 (dd, J = 6.73 Hz, 1H), 3.20 (brs, 1H), 3.41 –3.52 (m, 1H), 3.61 (d, J = 7.93 Hz 1H), 6.99 (brs, 1H), 7.1 (brs, 1H), 7.12–7.21 (m, 3H, Ar), 7.21 –7.3 (m, 2H, Ar), 7.56 (d, J = 7.17 Hz, 1H), 7.81 (d, J = 7.96 Hz, 1H), 8.10 (brs, 1H), 8.68 (brs, 1H); *HPLC analysis:* Jupiter 4  $\mu$ m Proteo 90 Å LC Column  $100 \times 2$  mm, 220 nm (t = 0-5 min, 80% A, 20% B; t = 5-45 min, 20% A, 80% B, t = 46 min, 100% B. (A = water, 0.1% TFA, B = methanol). flow rate = 0.5 mL/min,  $t_R$ =30.36 min); HRMS (ESI): Calcd for  $C_{31}H_{42}N_5O_6$ : m/z,  $[M + H]^+$  389.2553 Found: 389.2553.

#### **Inverse Virtual Screening**

The chemical structure of **1** was built and processed with Macromodel 8.5 (Schrödinger, LLC, New York, 2003). Molecular mechanics/dynamics calculations were performed on a quad-core Intel Xeon 3.4 GHz using Macromodel 8.5 and the OPLS force field. The Monte Carlo multiple minimum (MCMM) method (5000 steps) was used first to allow a full exploration of the conformational space. Molecular dynamics simulations were performed at 600 K and with a simulation time of 10 ns. A constant dielectric term, mimicking the presence of the solvent, was used in the calculations to reduce artifacts. Finally, an optimization (Conjugate Gradient, 0.05 Å convergence threshold) of the structures was

applied for the identification of a possible three-dimensional starting model of **1** for the subsequent steps of docking calculations. The panel of protein targets was prepared by a search of crystallized structures in the Protein Data Bank (Tables S3–S4, Supporting Information). Water molecules were removed, and polar hydrogens were added with AutodockTools 1.4.5. Molecular docking calculations were performed using Autodock-Vina software, using an exhaustiveness of 64. The selected grids focused on presumed sites of pharmacological interest on the basis of the binding modes of crystallized ligands in the PDB files wherever possible (Table S4, Supporting Information).

A more accurate analysis of the interaction between 1 vs. CPA was conducted with the Autodock 4.2 software package. To have an accurate weight of the electrostatics, we derived the partial charge of Zn=1.136 and of the amino acids involved in the catalytic center by DFT calculations at the B3LYP level by the 6–31G(d) basis set and ChelpG $^{34}$  method for population analysis (Gaussian 03 Package software $^{35}$ ). Ten calculations consisting of 256 runs were performed, obtaining 2560 structures (256  $\times$  10). The Lamarckian genetic algorithm was used for dockings. An initial population of 450 randomly placed individuals, a maximum number of 10.0  $\times$  10<sup>6</sup> energy evaluations, and a maximum number of 8.0  $\times$  10<sup>6</sup> generations were taken into account. A mutation rate of 0.02 and a crossover rate of 0.8 were used. Results differing by less than 3.0 Å in positional root-mean-square deviation (rmsd) were clustered together. For all the investigated compounds, all open-chain bonds were treated as active torsional bonds. Autodock Vina results were analyzed with Autodock Tools 1.4.5.

## **Supplementary Material**

Refer to Web version on PubMed Central for supplementary material.

# **Acknowledgments**

This work was supported by the NIH Intramural Research Program (NIDDK) and FARB (University of Salerno).

#### **Abbreviations**

CPA carboxypeptidase A
CPU carboxypeptidase U
DIC diisopropylcarbodiimide
DIPEA N,N-diisopropylethylamine

**FDLA** 1-fluoro-2,4-dinitrophenyl-5-leucinamide

**HBTU** O-benzotriazole-N,N,N',N'-tetramethyl-uronium-hexafluoro-phosphate

**HOBt** hydroxybenzotriazole

**PyBOP** benzotriazol-1-yl-oxytripyrrolidinophosphonium hexafluorophosphate

**PyBrOP** bromo-tris-pyrrolidino phosphoniumhexafluorophosphate

**TAFIa** activated thrombin-activable fibrinolysis inhibitor

#### References

1. Blunt JW, Copp BR, Munro MH, Northcote PT, Prinsep MR. Marine natural products. Nat. Prod. Rep. 2011; 28:196–268. [PubMed: 21152619]

2. Feling RH, Buchanan GO, Mincer TJ, Kauffman CA, Jensen PR, Fenical W. Salinosporamide A: a highly cytotoxic proteasome inhibitor from a novel microbial source, a marine bacterium of the new genus salinospora. Angew. Chem., Int. Ed. Engl. 2003; 42:355–357. [PubMed: 12548698]

- 3. Manzanares I, Cuevas C, Garcia-Nieto R, Marco E, Gago F. Advances in the chemistry and pharmacology of ecteinascidins, a promising new class of anti-cancer agents. Curr. Med. Chem.: Anti-Cancer Agents. 2001; 1:257–276.
- Mayer AMS, Glaser KB, Cuevas C, Jacobs RS, Kem W, Little RD, McIntosh JM, Newman DJ, Potts BC, Shuster DE. The odyssey of marine pharmaceuticals: a current pipeline perspective. Trends Pharmacol. Sci. 2010; 31:255–265. [PubMed: 20363514]
- Taori K, Paul VJ, Luesch H. Structure and activity of largazole, a potent antiproliferative agent from the Floridian marine cyanobacterium *Symploca* sp. J. Am. Chem. Soc. 2008; 130:1806–1807.
   [PubMed: 18205365]
- Villa FA, Gerwick L. Marine natural product drug discovery: Leads for treatment of inflammation, cancer, infections, and neurological disorders. Immunopharm. Immunotox. 2010; 32:228–237.
- Plaza A, Keffer JL, Bifulco G, Lloyd JR, Bewley CA. Chrysophaentins A-H, antibacterial bisdiarylbutene macrocycles that inhibit the bacterial cell division protein FtsZ. J. Am. Chem. Soc. 2010; 132:9069–9077. [PubMed: 20536175]
- 8. Plaza A, Gustchina E, Baker HL, Kelly M, Bewley CA, Mirabamides A-D. depsipeptides from the sponge *Siliquariaspongia mirabilis* that inhibit HIV-1 fusion. J. Nat. Prod. 2007; 70:1753–1760. [PubMed: 17963357]
- 9. Plaza A, Baker HL, Bewley CA. Mirabalin, [corrected] an antitumor macrolide lactam from the marine sponge *Siliquariaspongia mirabilis*. J. Nat. Prod. 2008; 71:473–477. [PubMed: 18271553]
- Matsunaga S, Fusetani N, Kato Y, Hirota H. Aurantosides A and B: cytotoxic tetramic acid glycosides from the marine spong *Theonella* sp. J. Am. Chem. Soc. 1991; 113:9690–9692.
- 11. Harada K, Fujii K, Hayashi K, Suzuki M, Ikai Y, Oka H. Application of D,L-FDLA derivatization to determination of absolute configuration of constituent amino acids in peptide by advanced Marfey's method. Tetrahedron Lett. 1996; 37:3001–3004.
- Rouhiainen L, Jokela J, Fewer DP, Urmann M, Sivonen K. Two alternative starter modules for the non-ribosomal biosynthesis of specific anabaenopeptin variants in Anabaena (Cyanobacteria). Chem. Biol. 2010; 17:265–273. [PubMed: 20338518]
- 13. Walther T, Arndt HD, Waldmann H. Solid-support based total synthesis and stereochemical correction of brunsvicamide A. Org. Lett. 2008; 10:3199–3202. [PubMed: 18590275]
- Kobayashi J, Sato M, Ishibashi M, Shigemori H, Nakamura T, Ohizumi Y, Keramamide A. a novel peptide from the Okinawan marine sponge *Theonella* sp. J. Chem. Soc., Perkin Trans. 1991; 1:2609–2611.
- 15. Kobayashi J, Sato M, Murayama T, Ishibashi M, Walchi MR, Kanai M, Shoji J, Ohizumi Y. Konbamide, a novel peptide with calmodulin antagonistic activity from the Okinawan marine sponge *Theonella* sp. J. Chem. Soc., Chem. Commun. 1991; 3:1050–1052.
- Schmidt EW, Harper MK, Faulkner DJ. Mozamides A and B, cyclic peptides from a theonellid sponge from mozambique. J. Nat. Prod. 1997; 60:779–782.
- 17. Uemoto H, Yahiro Y, Shigemori H, Tsuda M, Takao T, Shimonishi Y, Kobayashi J. Keramamides K and L, new cyclic peptides containing unusual tryptophan residue from *Theonella* sponge. Tetrahedron. 1998; 54:6719–6724.
- 18. Marsh IR, Bradley M, Teague SJ. Solid-phase total synthesis of oscillamide Y and analogues. J. Org. Chem. 1997; 62:6199–6203.
- 19. Coste J, Le-Nguyen D, Castro B. PyBOP: A new peptide coupling reagent devoid of toxic by-product. Tetrahedron Lett. 1990; 31:205–208.
- 20. Harada K, Fujii K, Shimada T, Suzuki M, Sano H, Adachi K, Carmichael WW. 2 cyclic-peptides, anabaenopeptins, a 3rd group of bioactive compounds from the cyanobacterium *Anabaena-flos-aquae* Nrc-525-17. Tetrahedron Lett. 1995; 36:1511–1514.
- 21. Bubik A, Sedmak B, Novinec M, Lenarcic B, Lah TT. Cytotoxic and peptidase inhibitory activities of selected non-hepatotoxic cyclic peptides from cyanobacteria. Biol. Chem. 2008; 389:1339–1346. [PubMed: 18713022]

22. Gesner-Apter S, Carmeli S. Protease inhibitors from a water bloom of the cyanobacterium Microcystis aeruginosa. J. Nat. Prod. 2009; 72:1429–1436. [PubMed: 19650639]

- Van Wagoner RM, Drummond AK, Wright JL. Biogenetic diversity of cyanobacterial metabolites. Adv. Appl. Microbiol. 2007; 61:89–217. [PubMed: 17448789]
- Walther T, Renner S, Waldmann H, Arndt HD. Synthesis and structure-activity correlation of a brunsvicamide-inspired cyclopeptide collection. ChemBioChem. 2009; 10:1153–1162. [PubMed: 19360807]
- 25. Bunnage ME, Blagg J, Steele J, Owen DR, Allerton C, McElroy AB, Miller D, Ringer T, Butcher K, Beaumont K, Evans K, Gray AJ, Holland SJ, Feeder N, Moore RS, Brown DG. Discovery of potent & selective inhibitors of activated thrombin-activatable fibrinolysis inhibitor for the treatment of thrombosis. J. Med. Chem. 2007; 50:6095–6103. [PubMed: 17990866]
- 26. Rees DC, Lipscomb WN. Binding of ligands to the active site of carboxypeptidase A. Proc. Natl. Acad. Sci. U. S. A. 1981; 78:5455–5459. [PubMed: 6946483]
- Lauro G, Romano A, Riccio R, Bifulco G. Inverse virtual screening of antitumor targets: pilot study on a small database of natural bioactive compounds. J. Nat. Prod. 2011; 74:1401–1407. [PubMed: 21542600]
- 28. Trott O, Olson AJ. AutoDock Vina: improving the speed and accuracy of docking with a new scoring function, efficient optimization, and multithreading. J. Comput. Chem. 2010; 31:455–461. [PubMed: 19499576]
- 29. The top two hits corresponded to galectin 7 and calmodulin (CaM). Inspection of the docked models showed 1 to be located in the galactose binding site of galectin 7, anchored through the exocyclic Phe residue, and in an extensive hydrophobic channel in CaM, making only partial contacts with this site. Because these interactions were not optimal relative to the known ligands, we did not pursue them further.
- 30. Morris GM, Huey R, Lindstrom W, Sanner MF, Belew RK, Goodsell DS, Olson AJ. AutoDock4 and AutoDockTools4: Automated docking with selective receptor flexibility. J. Comput. Chem. 2009; 30:2785–2791. [PubMed: 19399780]
- 31. Rees DC, Lipscomb WN. Refined crystal structure of the potato inhibitor complex of carboxypeptidase A at 2.5 A resolution. J. Mol. Biol. 1982; 160:475–498. [PubMed: 7154070]
- 32. Roos E, Bernabe P, Hiemstra H, Speckamp N, Kaptein B, Boesten WHJ. Palladium-catalyzed transprotection of allyloxycarbonyl-protected amines: efficient one-pot formation of amides and dipeptides. J. Org. Chem. 1995; 60:1733–1741.
- 33. Mock WL, Liu Y, Stanford DJ. Arazoformyl peptide surrogates as spectrophotometric kinetic assay substrates for carboxypeptidase A. Anal. Biochem. 1996; 239:218–222. [PubMed: 8811913]
- 34. Breneman CM, Wiberg KB. Determining atom-centered monopoles from molecular electrostatic potentials. The need for high sampling density in formamide conformational analysis. J. Comput. Chem. 1990; 11:361–373.
- 35. Frisch, MJ.; Trucks, GW.; Schlegel, HB.; Scuseria, GE.; Robb, MA.; Cheeseman, JR.; Scalmani, G.; Barone, V.; Mennucci, B.; Petersson, GA.; Nakatsuji, H.; Caricato, M.; Li, X.; Hratchian, HP.; Izmaylov, AF.; Bloino, J.; Zheng, G.; Sonnenberg, JL.; Hada, M.; Ehara, M.; Toyota, K.; Fukuda, R.; Hawegawa, J.; Ishida, M.; Nakajima, T.; Honda, Y.; Kitao, O.; Nakai, H.; Vreven, T.; Montgomery, J,JA.; Peralta, JE.; Ogliaro, F.; Bearpark, M.; Heyd, JJ.; Brothers, E.; Kudin, KN.; Staroverov, VN.; Kobayashi, R.; Normand, J.; Raghavachari, K.; Rendell, A.; Burant, JC.; Iyengar, SS.; Tomasi, J.; Cossi, M.; Rega, N.; Millam, NJ.; Klene, M.; Knox, JE.; Cross, JB.; Bakken, V.; Adamo, C.; Jaramillo, J.; Gomperts, R.; Stratmann, RE.; Yazyev, O.; Austin, AJ.; Cammi, R.; Pomelli, C.; Ochterski, JW.; Martin, RL.; Morokuma, K.; Zakrzewski, VG.; Voth, GA.; Salvador, P.; Dannenberg, JJ.; Dapprish, S.; Daniels, AD.; Farkas, O.; Foresman, JB.; Ortiz, JV.; Cioslowski, J.; Fox, DJ. Wallingford, CT: 2009.



**Figure 1.** Structure of namalide (left) and key HMBC and ROE correlations (right).

4 L-Phe1, L-IIe, L-Lys, L-Phe25 L-Phe1, L-allo-IIe, D-Lys, L-Phe2

**Figure 2.** Synthetic Namalide Analogs.

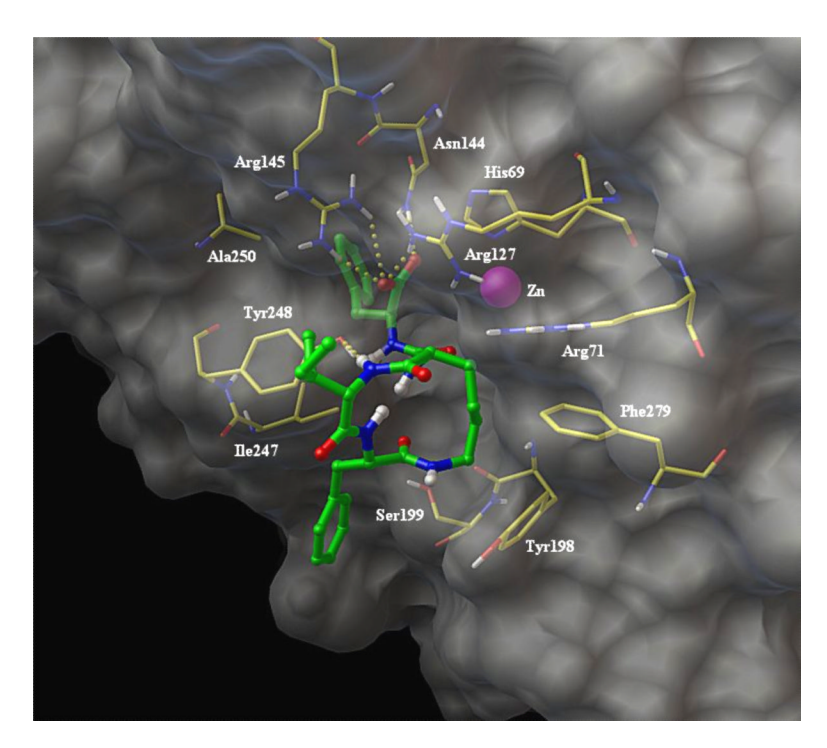


Figure 3. Docked model of 1 to CPA. Protein is shown as a grey surface,  $Zn^{2+}$  atom as a magenta sphere, and residues in contact with 1 as yellow (C atoms), blue (N atoms), red (O atoms), grey (H atoms)sticks; namalide (1) is rendered as green (C atoms), blue (N atoms), red (O atoms), grey (H atoms) sticks and balls.

$$HO_2C$$
 $HO_2C$ 
 $HO_2$ 

**Scheme 1.** Retrosynthesis of Namalide (1).

**Scheme 2.** Solid Phase Synthesis of Namalide (1).

 $\label{eq:Table 1} \mbox{Table 1} \mbox{NMR Spectroscopic Data for Namalide (1) in $CD_3OD$.}$ 

|        | 1                |   |                         |  |
|--------|------------------|---|-------------------------|--|
|        | δ c <sup>a</sup> | $\delta_{\mathrm{H}}^{}} b}(J \text{ in Hz})$ | $HMBC^c$                |  |
| Lys    |                  |   |                         |  |
| 1      | 175.6            |   |                         |  |
| 2      | 56.3             | 4.00 m  | $1, 1_{Urea}$           |  |
| 3      | 30.8             | 1.76, 1.68, m                                 | 2                       |  |
| 4      | 20.1             | 1.30, 1.10, m                                 |                         |  |
| 5      | 30.2             | 1.61, 1.30, m                                 |                         |  |
| 6      | 38.2             | 3.63, 2.86, m                                 | $4, 5, 1_{phe1}$        |  |
| Phe1   |                  |   |                         |  |
| 1      | 172.9            |   |                         |  |
| 2      | 55.9             | 4.57 <sup>d</sup>                             | $1,3, 1_{Ile}$          |  |
| 3      | 37.0             | 3.18, 2.96, m                                 | 1, 2, 1', 2'            |  |
| 1'     | 139.0            |   |                         |  |
| 2', 6' | 130.6            | $7.25^{d}$                                    |                         |  |
| 3', 5' | 129.1            | $7.22^{d}$                                    |                         |  |
| 4'     | 127.2            | $7.17^{d}$                                    |                         |  |
| Ile    |                  |   |                         |  |
| 1      | 173.7            |   |                         |  |
| 2      | 61.3             | 3.95 br s                                     |                         |  |
| 3      | 35.5             | 1.70 m  |                         |  |
| 4      | 26.2             | 1.48, 1.06 m                                  |                         |  |
| 5      | 10.0             | 0.80 t (7.5)                                  | 3, 4                    |  |
| Me-3   | 15.3             | 0.54 (6.7)                                    | 2, 3                    |  |
| Urea   |                  |   |                         |  |
| 1      | 159.4            |   |                         |  |
| Phe2   |                  |   |                         |  |
| 1      | 178.6            |   |                         |  |
| 2      | 57.5             | 4.42, m                                       | 1, 3, 1 <sub>Urea</sub> |  |
| 3      | 39.8             | 3.15, 3.06 m                                  | 1 1', 2'                |  |
| 1'     | 139.6            |   |                         |  |
| 2', 6' | 130.7            | 7.23 <sup>d</sup>                             |                         |  |
| 3', 5' | 129.2            | 1.22 <sup>d</sup>                             |                         |  |
| 54     | 127.6            | 1.16 <sup>d</sup>                             |                         |  |

 $<sup>^{</sup>a}\mathrm{Recorded}$  at 125 MHz; referenced to residual CD3OD at d 49.1 ppm.

 $<sup>^</sup>b\mathrm{Recorded}$  at 500 MHz; referenced to residual CD3OD at d 3.30 ppm.

 $^{\it C}\!\!$  Proton showing HMBC correlation to indicated carbon.

 $^d\mathrm{Overlapping}$  signals.

#### Table 2

# Inhibition of CPA<sup>a</sup>

| Peptide | IC <sub>50</sub> (μM)             |  |  |
|---------|-----------------------------------|--|--|
| 1       | $0.25 \pm 0.03$                   |  |  |
| 3       | na <sup>b</sup>                   |  |  |
| 4       | na <sup>b</sup>                   |  |  |
| 5       | $\operatorname{nt}^{\mathcal{C}}$ |  |  |
| 6       | $4.5 \pm 0.9$                     |  |  |
| 7       | na <sup>b</sup>                   |  |  |

 $<sup>^{</sup>a}$ Tested in duplicate;

b not active at 30 μM;

 $<sup>^{</sup>c}$  poor reproducibility and solubility